Title: Global change adaptation reduces plasticity and limits future resilience

Authors: Reid S. Brennan[†1]*, James A. deMayo[†2], Hans G. Dam[2], Michael Finiguerra[3], Hannes Baumann[2], Melissa H. Pespeni[1]*

Affiliations:

[1]Department of Biology, University of Vermont, Burlington, VT, USA

[2]Department of Marine Sciences, University of Connecticut, Groton, CT, USA

[3]Department of Ecology and Evolutionary Biology, University of Connecticut, Groton, CT, USA

*Correspondence to: Reid.Brennan@uvm.edu; mpespeni@uvm.edu

[†]Authors contributed equally to this work

Abstract: Species may persist through the unprecedented changes in global conditions using genetic adaptation or physiological plasticity. However, few empirical studies have revealed the relationship between adaptation and plasticity or addressed the long-standing debate on whether plasticity impedes or facilitates adaptive evolution. Here, we used experimental evolution and reciprocal transplantation of the marine coastal copepod, *Acartia tonsa*, to present-day and future greenhouse conditions (high temperature, high CO_2). Despite the presence of plasticity in ambient conditions, twenty generations of selection resulted in highly parallel genetic adaptation to greenhouse conditions where genes related to stress response, actin regulation, developmental processes, and energy production diverged between conditions. Genetic adaptation, however, reduced fecundity and population growth when greenhouse animals were returned to ambient conditions or reared in low food conditions. Concurrently, adaptation reduced gene expression plasticity by 12.7 fold. Despite the loss of plasticity, across three successive transplant generations, greenhouse-adapted animals were able to match the ambient-adaptive transcriptional

profile through genetic adaptation, which in turn eroded nucleotide diversity in greenhouse-adaptive genes. These results demonstrate the power of experimental evolution from natural populations to reveal the mechanisms, timescales of responses, consequences, and reversibility of complex, physiological adaptation. While plasticity facilitated initial survival in global change conditions, it eroded after 20 generations as populations genetically adapted, limiting resilience to new stressors and previously benign environments.

Main Text: Though global conditions are changing at a geologically unprecedented rate and the frequency of extreme events is increasing [1], species can use genetic adaptation or physiological plasticity to persist [2–4]. Genetic adaptation, defined as heritable genetic change that improves population fitness in an environment [5], enables resilience by shifting population phenotypes to tolerate different conditions. Selection for adaptive phenotypes can shift population genetic variation over short time scales, as few as one to four generations [6–9]. Conversely, plasticity allows a single genotype to generate different phenotypes in response to the environment within a generation [10]. Considering rapid changes in environmental conditions, adaptive plasticity enables organisms to maintain fitness across environments [11] through underlying phenotypic, physiological, or gene expression changes [12]. However, the interaction and relative contributions of genetic adaptation and plasticity to population persistence in rapid environmental change is not well understood [13–16]. Plasticity may inhibit adaptation by shielding genetic variation from natural selection, but more recent work has indicated that plasticity can precede and facilitate adaptation to novel environments [17–20]. Thus, while adaptation and plasticity are not always antagonistic, there is limited empirical support and the consequence of this process on the resilience of populations is unclear [21].

Some species may be more equipped to survive environmental changes using either or both genetic adaptation or plasticity [2]. Organisms that live in dynamic environments, have distributions that span a wide range of environmental conditions, and are highly dispersing are predicted to have the greatest capacity to respond to rapid environmental change [22,23]. These characteristics support the maintenance of both standing genetic variation, which enables adaptation, and physiological plasticity [24,25]. Many marine species live in environments that vary across time and space and have life histories that promote dispersal [26,27]. This is true of copepods, the most abundant marine metazoan [28] which have been shown to have plasticity and genetic variation for adaptation to global change conditions [29–31]. Despite their ecological importance, there is limited empirical evidence of adaptive capacity to global change conditions over longer timescales in natural populations of copepods, or any metazoan [32,33], and the relationship between plasticity and genetic adaptation is not well understood in these systems[34].

Experimental evolution is a particularly powerful approach to understand resilience as organisms can be exposed to specific selective pressures over multiple generations [35]. From this, one can identify both the adaptive potential and the mechanisms of adaptation of a population, directly providing insight into how a population may cope with changing climates [36]. Here, we use 20 generations of experimental evolution to greenhouse (high CO_2, temperature) and present-day ambient conditions followed by three generations of reciprocal transplantation. Experimental evolution and reciprocal transplantation allow us to mimic both chronic environmental changes and extreme events, respectively, to understand the interplay of rapid adaptation and plasticity

and to explore associated costs of adaptation, particularly those relating to reductions of genetic diversity and plasticity.

We experimentally evolved the globally distributed, foundational copepod species, *Acartia tonsa,* to ambient and global change conditions. As a dominant prey item for forage fish, *A. tonsa* serves as a critical link in the marine food web, supporting economically important fisheries [37] and as major phytoplankton grazers, copepods substantially contribute to the storage of atmospheric CO_2 and thus mediate marine biogeochemical cycles [38]. Replicate cultures (4 replicates per condition, ~4,000 individuals per replicate) of *A. tonsa* were subjected to 20 generations of selection in ambient (AM: 400 ppm pCO_2 and 18ºC) and combined high CO_2 × temperature (greenhouse, GH: 2000 ppm pCO_2 and 22ºC) conditions followed by three generations of reciprocal transplantation of both lines to opposite conditions (Fig. 1). These treatments were chosen as they represent present-day and a worst case, yet realistic scenario [39,40]; in the coming century, global mean ocean surface temperatures will increase by 2-4 ºC[41] and oceanic CO_2 concentrations will potentially reach 2000 ppm by the year 2300 [42]. Reciprocal transplant represents rapid responses to environmental change and extreme events. We denote evolved lines with their abbreviation and the treatment condition during transplant as a subscript (i.e., AM_{GH} = ambient line transplanted to greenhouse conditions). Fecundity and survival were measured immediately following transplant for all cultures. Because costs may only be evident in the face of additional stressors, we also measured fecundity and survival under limited food availability, which is a potential consequence of climate change for marine environments[43]. RNA was collected from pools of 20 adults from each of four replicate cultures at the first, second, and third generation after transplant for both experimentally evolved and transplanted lines (Fig. 1).

We estimated allele frequencies at 322,595 variant sites with at least 50× coverage across all samples and quantified transcript abundance for an average 24,112 genes. We test for evidence of adaptation, identify underlying mechanisms and potential costs associated with adaptation at the organismal, physiological, and genetic levels of organization, and use reciprocal transplants to test how plasticity and genetic adaptation interact during short- and longer-term responses to global change conditions.

Results and discussion

Organismal, transcriptomic, and genomic evidence indicate that selection shaped the phenotypes and genotypes in the replicate lines after 20 generations in greenhouse conditions (Figs. 2 & 3). Whole organism performance showed that fecundity was equally high for both lines in their home environments but declined for GH lines after transplant to AM conditions (48% reduction in egg production relative to GH_{GH} ; $P < 0.02$; Fig. 2A). In contrast, transplanted AM_{GH} demonstrated sufficient plasticity to alter their physiology to maintain similarly high egg production as the non-transplanted lines (Fig. 2A). Considering that AM individuals represent the non-selected, control populations, the reduced fecundity of GH populations transplanted to previously benign AM conditions represents a loss of ancestral plasticity.

In contrast to egg production, survivorship from *nauplii* to reproductive maturity was 60% lower for greenhouse compared to ambient lineages regardless of the environment or food regime ($P <$ 0.001; Fig. 2B). However, fitness (the net reproductive rates), estimated by using fecundity, development rates, reproductive timing, and survival [44], were stable for food replete GH_{GH} and AM lines in both conditions (Fig. 2C). The high fitness for AM lines across environments again

115 demonstrates sufficient plasticity to alter underlying physiology. In contrast, GH_{AM} transplant
116 populations exhibited decreased net reproductive rates relative to GH_{GH} animals ($P = 0.01$, Fig.
117 2C), indicating adaptation to GH conditions. In addition, population growth depended on
118 condition (marginally significant line x treatment interaction, $P = 0.056$ Fig. 2C), suggesting a
119 loss of the ability in GH lines to maintain high fitness across environments and a loss of
120 physiological plasticity to tolerate the different conditions. The steady-state growth rate when
121 food is non-limiting of GH_{GH} populations despite decreased survival relative to AM lines (Fig.
122 2B) was due to compensation via higher egg production relative to GH_{AM} populations (Fig. 2A),
123 faster development, and earlier reproductive timing in GH conditions. Taken together, the
124 constant population growth in GH conditions and the reduction in egg production following
125 transplant to AM conditions suggest that there was strong directional selection in greenhouse
126 conditions that resulted in adaptation and the maintenance of high egg production that came at
127 the cost of maintaining plasticity to tolerate previously benign, ambient conditions.
128
129 We also explored the ability of lines to tolerate an additional stressor, low food availability, to
130 determine resilience to tolerate environmental fluctuations. GH animals performed poorly under
131 low food availability regardless of environment (Fig. 2). Under low food, relative to AM lines,
132 GH lines experienced a 67% reduction in egg production rates ($P < 0.001$; Fig. 2A), 70%
133 reduction in survival ($P < 0.001$; Fig. 2B), and a 40% reduction in fitness ($P < 0.001$; Fig. 2C).
134 Thus, selection in greenhouse conditions may result in animals less resilient to further nutritional
135 limitations [45], which is likely driven by increased energetic costs leading to increased stress [46].
136

To understand the genetic and physiological mechanisms driving the observed decreases in plasticity and performance in GH animals, we tested for changes in allele frequencies (322,595 loci) and gene expression (24,927 genes) among AM and GH lines in their home environments. We found consistent, directional divergence in allele frequencies between replicate GH and AM lines, indicating that selection resulted in adaptation to GH conditions (Fig. 3 A, B, S1, S2). 17,720 loci (5.5% of all loci with >50X coverage) showed consistent allele frequency divergence, suggesting that adaptation to global change condition is highly polygenic (GH_{GH} versus AM_{AM}; Cochran–Mantel–Haenszel test FDR corrected significance threshold: 5.17e-08) [47–49]. 1,876 genes (7% of genes surveyed) showed differential expression between control and experimentally evolved replicate lines in their home environment (GH_{GH} versus AM_{AM}; $P <$ 0.05). Of potential candidate genes driving adaptation (Fig. S2), one gene, NADH-ubiquinone oxidoreductase 49 kDa subunit (NDUFS2), was an extreme outlier for divergence in allele frequencies, 77%, which is 72% greater than the global average (5%; Fig. S3). NDUFS2 is a nuclear-encoded, core subunit of Complex 1 of the mitochondrial electron transport chain (ETC) that has been shown to be inhibited by heat stress [50,51]. The three substitutions identified here were all non-synonymous, including a non-polar Isoleucine to polar Asparagine, in linkage disequilibrium (Fig. S2), and in a single alpha helix of the ETC subunit. This alternative NDUFS2 haplotype targeted by selection could improve energy production under heat stress for global change-adapted copepods, a hypothesis worth future functional investigation.

We found substantial overlap in the functional classes of genes that had evolved allelic and expression differences; shared categories included response and detection of stress and stimuli, developmental processes, actin organization and regulation, and proteolytic processes (Fig. 3C,

D; Tables S1, S2). These functions likely relate to increased survival in warmer and more acidic conditions. For example, proteolysis is integral to the stress response [52] while actin modifications have been repeatedly identified as targets of pH adaptation and resilience [9,53] and are linked to cytoskeleton maintenance that is responsive to low pH stress in copepods [54]. Despite shared functions, there was little overlap in the specific genes that evolved allelic and adaptive expression differences (16%; Fisher's exact test; $P > 0.05$), suggesting that adaptive divergence in protein function and gene expression targeted different, but functionally related genes. Similarly, we found no correlation between the degree of expression and allelic responses (Fig. S4; $R^2 = 0.002$), suggesting no impact of potential allele-biased expression on estimates of allele frequencies from pools of sequenced RNA. However, we found strong allele frequency divergence in regulators of expression, predominantly in genes relating to RNA processing (Fig. 3C) and also ribosomal S6 kinase, a gene involved in the regulation of numerous transcription factors and translation (Fig. S2) [55]. Taken together, these results suggest that regulators of gene expression were under selection and responsible for the adaptive changes in gene expression.

We next quantified gene expression plasticity to understand if rapid adaptation has resulted in a loss of physiological plasticity. We identify plastic changes in gene expression for GH and AM lines by comparing expression in the home environment after 20 generations to short-term gene expression responses after transplantation (GH_{GH} vs. GH_{AM}; AM_{AM} vs. AM_{GH}; Fig. 4A). At the first generation of transplant, AM_{GH} was plastic in expression for 4,719 genes (Padj< 0.05; 20% of genes), a 12.7 fold greater response than GH_{AM} (372 genes; 1.6 % of genes). However, by the second and third generations' transplant, this difference diminished due to the relative increase of GH gene expression changes (F2: 4.5%; F3: 4.1%) and decrease of AM changes (F2: 1.7%; F3:

6.3%). While expression changes at F1 were likely due to plasticity, differential gene expression at F2 and F3 could be due to plasticity or evolution, a question we address below.

In accord with the lower overall plasticity for GH animals at F1, AM animals showed a significantly greater match to the adaptive expression profile than GH (Discriminant analysis of principal components (DAPC); $P = 0.03$; Fig. 4B). Discriminant function space was generated from AM_{AM} and GH_{GH}, representing the adaptive expression differences after 20 generations in each environment. Transplanted lines were fit to this discriminant function space to determine if and how expression changed to match the adaptive expression profile where the adaptive plasticity is summarized by the length of each line in Fig. 4. Despite lower plasticity in adaptive gene expression for GH animals at F1, AM and GH lines demonstrated similar shifts at F2 and F3 where lines converge on the adaptive expression profile by the F3 generation (Fig. 4B). Alternative methods based on DeSeq2 differential expression recapitulate these adaptive expression shifts (Fig. S5). This increase in adaptive gene expression across generations indicates that copepods, even after 20 generations of experimental evolution in ambient or greenhouse conditions and despite differences in initial levels of plasticity, were able to match adaptive gene expression profiles increasingly with each successive generation.

We used a similar DAPC approach to test if allele frequencies changed to match adaptive allele frequencies following transplant and to explore whether gene expression changes at F2 and F3 were due to plasticity or evolution (Fig. 4C). Allele frequencies of non-transplanted lines were used to generate discriminate function space and the shifts of transplanted lines indicated the degree of adaptive evolution following transplant. This quantified the degree to which

transplanted lines evolved using the same alleles that adaptively evolved over the initial 20 generations. At generations F1 and F2, allele frequency changes were similar between AM and GH lines (Markov chain Monte Carlo (MCMC) generalized linear mixed model; $P_{MCMC} > 0.05$; Fig. 4C). However, by F3 GH animals showed significantly greater adaptive evolution than AM ($P_{MCMC} = 0.02$). These findings were again mirrored by an independent analysis based on Cochran–Mantel–Haenszel tests (Fig. S5). Together with the gene expression analysis, these results indicate that AM_{GH} animals were able to match the greenhouse adaptive transcriptional profiles without changes in allele frequencies but rather through physiological and/or transgenerational plasticity. Conversely, the GH_{AM} animals had lost the plasticity necessary to transcriptionally respond and matched the adaptive transcriptional profile through evolution, i.e., selection drove changes in allele frequencies across the three generations of transplant.

Rapid adaptation can result in a selective bottleneck which could drive a loss of genetic diversity during long-term selection or short-term transplant. To test this hypothesis, we quantified nucleotide diversity (π) for each treatment following 20 generations of selection and after transplant. Remarkably, we found no significant loss of genetic diversity after long-term adaptation to greenhouse conditions (GH_{GH}, Fig. 5A, $P_{Tukey} > 0.05$). Similarly, ambient lines, both transplanted and not, maintained high levels of genetic diversity ($P_{Tukey} > 0.05$). However, when transplanted back to ambient conditions, GH_{AM} showed a significant drop in diversity by F3 ($P_{Tukey} < 0.05$; Fig. 5A), indicating a global loss of genetic diversity. This suggests that the successive shifts in allele frequency after transplant of GH to AM (GH_{AM}; Fig. 4C) resulted in a loss of genetic diversity (Fig. 5A). To test if this loss of genetic diversity in transplant from GH to AM was concentrated in specific regions of the genome, we compared changes in nucleotide

diversity in regions identified as adaptively diverged between greenhouse and ambient lines (i.e., regions containing 17,720 consistently divergent loci) versus all other loci ("non-adaptive"). For GH_{AM} lines, the loss of nucleotide diversity was concentrated in genomic regions containing adaptive loci (Fig. 5B; Wilcoxon test $P = 0.005$), while there was no loss of diversity in AM_{GH} lines as a control contrast (Fig. 5B; $P = 0.11$). In addition, the loss of nucleotide diversity for GH_{AM} lines was concentrated in genes with functions related to sequestration of actin monomers, cytokinesis, and response to stress (Fig. 5C; Table S3), similar to those underlying adaptive genetic divergence between AM_{AM} and GH_{GH} lines (Table S1). The lack of nucleotide diversity loss for AM_{GH} lines and the absence of functional enrichment indicates that selection did not act on these transplanted lines; this is consistent with the sustained ability for a plastic response. These results also suggest that the loss of genetic diversity for GH_{AM} was due to selection following their loss of physiological plasticity after long-term adaptation to greenhouse conditions.

Conclusion

Whether plasticity promotes or constrains adaptation has been a long-standing debate [13], and only a few recent studies have provided empirical evidence that plasticity can promote adaptation [17–20]. We reveal a complex interaction between plasticity and adaptation in response to global change conditions. In the short-term, three generations, plasticity buffered populations from environmental change allowing AM lines to tolerate greenhouse conditions through plasticity. Over the longer-term, 20 generations, plasticity to acclimate was lost as adaptation to greenhouse conditions proceeded, indicating costs to maintain plasticity [56]. Our results provide

evidence that plasticity does not constrain genetic adaptation but, over time, genetic adaptation erodes plasticity.

This interplay between plasticity and adaptation has important implications for our understanding of mechanisms of species persistence to global change conditions. We demonstrate that copepods have the capacity to adapt over 20 generations, approximately one year, using the standing genetic variation that exists in natural populations. However, reciprocal transplant and food challenges revealed significant costs of this adaptation; populations lost physiological plasticity, the ability to tolerate food limitation, and ultimately adaptive genetic variation for greenhouse conditions. Given the increasing frequency of extreme environmental conditions, rapid adaptation of *A. tonsa* to a temporary extreme may result in a population that is maladapted when conditions return to the previous state. Thus, while plasticity may enable persistence initially, adaptation can drive a loss of plasticity that can lead to reduced resiliency when environmental conditions fluctuate further. These results demonstrate the utility of experimental evolution in understanding complex adaptation in natural systems and to reveal the mechanisms, time-scales of responses, consequences, and reversibility of this process. As we begin to incorporate adaptive potential and plasticity into species persistence models [57–60], these results caution that, even for species predicted to be resilient to rapid global change, there may be costs to adaptive evolution.

Methods

Experimental set-up

Copepods (n=1,000) were collected in June of 2016 from Esker Point Beach in Groton, CT, USA (decimal degrees: 41.320725, -72.001643) and raised for at least three generations prior to the start of transgenerational adaptation to limit maternal effects [61]. Parental individuals were acclimated to one of two experimental conditions: 1) AM – Ambient temperature (18 ˚C), Ambient CO_2 (~400 ppmv CO_2, pH ~8.2) or 2) GH – High temperature (22 ˚C), high CO_2 (~2000 ppmv CO_2, pH ~7.5). Cultures were fed every 48-72 hours at food-replete concentrations of carbon (>800 µg C/L) split equally between three species of prey phytoplankton. Prey phytoplankton included *Tetraselmis* spp., *Rhodomonas* spp., and *Thalassiosira weissflogii*, which is a common diet combination used for rearing copepods[62]. About 400 females and 200 males were used to seed each treatment, yielding an estimated 15,000 eggs and newly hatched *nauplii* for the initial F0 generation. Four replicate cultures per treatment were maintained in individual 3L culture containers with two treatments per environment (eight cultures per environment). Each environment was housed in one of two identical incubators. Elevated CO_2 levels were achieved with two-gas proportioners (Cole-Parmer, Vernon Hills, IL, USA) combining air with 100% bone dry CO_2 that was delivered continuously to the bottom of each replicate culture. Actual measurements of experimental CO_2 were determined based on measurements of salinity, temperature, pH, and total alkalinity using CO_2Sys. Total alkalinity was measured before and after the course of the experiment. Seawater was filtered to 30 µm and measured immediately using an endpoint titration as described previously [63]. Target pH values were monitored daily using a handheld pH probe (Orion Ross Ultra pH/ATC Triode with Orion Star A121 pH Portable Meter (Thermo FisherScientific®, Waltham, MA, USA). Continuous bubbling maintained higher than necessary dissolved oxygen levels (>8 mg/L). To assess functional life-history traits, smaller volume experiments were housed in the same temperature-

296 controlled incubators in custom plexiglass enclosures with the atmosphere continuously flooded
297 with CO_2 infused air at the appropriate concentration, which allows for passive diffusion of CO_2
298 into the experiments. Copepods were raised in the respective two experimental treatments for 20
299 generations before the reciprocal transplant.
300
301 *Reciprocal transplant*
302 At the 21st generation, we performed a reciprocal transplant between copepods from AM and
303 GH. Each of the four replicates from each treatment was split to yield four additional replicates
304 for each of two new transplant treatments: AM_{GH} and GH_{AM} (as well as sham transfers: AM_{AM}
305 and GH_{GH}). Copepods were raised for three subsequent generations and were fed every 48-72
306 hours as described above. This design lead to 48 total cultures: 2 treatments × 2 transplant/non-
307 transplant × 4 replicates × 3 generations.
308
309 *Life-history traits*
310 Day-specific survivorship was measured every 48-72 hours, with food media replaced on
311 monitoring days. Food media was provided at the appropriate food concentration (>800 µg C/L
312 for food-replete and 250 µg C/L for food-limited) divided in equal carbon proportions between
313 the three afore-mentioned prey species in 0.2 µm filtered seawater collected from Long Island
314 Sound. Food media was acclimated to the appropriate temperature and CO_2 concentration prior
315 to replacement. Survivorship was assessed among twelve 250-mL beakers per treatment (3 food
316 concentrations × 4 replicates = 12 beakers per treatment) containing 25 individual N1 *nauplii*
317 and monitored until sexual maturity (adulthood) Log rank analysis of survivorship was assessed
318 using the survival [64,65] and survminer [66] packages in R.

Egg production rate (EPR) and hatching frequency (HF) were assessed with 36 individual mate pairs of newly matured adults per treatment (12 pairs per food concentration × 3 food concentrations = 36 pairs per treatment) divided evenly between four replicates within a treatment. Adults were incubated in 25 mL petri dishes (FisherScientific, Waltham, MA, USA) over three days in the same temperature-controlled incubators and plexiglass enclosures described above. After the initial three-day incubation, adults were assessed for survival and removed to avoid cannibalization of eggs. Eggs were allowed to hatch over a subsequent three-day incubation. Food media was prepared as described for survivorship and replaced daily during egg laying to ensure accurate food concentrations were near saturation and not reduced due to daily grazing [67]. Lids of petri dishes were left off-center to allow for full contact with the atmosphere and diffusion of CO_2. Plates with dead males were still evaluated for EPR, but not HF. Plates with dead females were not evaluated. After the hatching period, plates were preserved with non-acid Lugol's solution and quantified. Per capita EPR was calculated as $(E_u+E_h)/t$ where E_u represents unhatched eggs, E_h represents hatched eggs (*nauplii*), and t represents egg laying time. Hatching frequency was calculated as $E_h/(E_u+E_h)$.

The population net reproductive rate, λ, was calculated as the dominant eigenvalue of an assembled projected age-structured Leslie Matrix constructed from survivorship and fecundity data [44]. Briefly, day-specific probabilities of survivorship are calculated from day-specific survivorship as $P_x = \frac{l_x}{l_{x-1}}$ where l_x represents the individuals on day x and l_{x-1} represents the number of individuals on day $x-1$. Probabilities of survivorship on day 1 are assumed to be 100% or a proportion of 1. Per capita EPR and HF are calculated as described above, with fecundity

rates equaling the product of EPR and HF. Because only females produce offspring, total fecundity rates must be scaled to the sex ratio (ratio of females:males) observed in survivorship experiments. To account for differences in individual development time for each treatment, fecundity rates are assigned to all days after the first matured adult is observed. We assume that survivorship in each beaker is equally as likely to experience the fecundity values observed in EPR experiments. Therefore, each mate-pair fecundity rate was paired with each survivorship beaker to construct a matrix. This yields a maximum of 48 matrices per treatment per food concentration (4 beakers × 12 mate pairs).

We constructed linear mixed models with line, environment, and food concentration as fixed effects with all interactions, and culture replicate as a random effect. Two post-hoc tests were conducted. First, to quantify differences in plasticity between the lines, we evaluated genotype × environment interactions on life-history traits separately for each food concentration. Second, post-hoc t-test comparisons were used to conduct pairwise comparisons of the interactions for each life history trait.

Genomics

RNA from pools of 20 individuals was extracted using TRIzol reagent (Invitrogen, Carlsbad, CA, USA) and purified with Qiagen RNeasy spin columns (Qiagen, Germantown, MD, USA). RNAseq libraries were prepared by Novogene (Sacramento, CA, USA) and sequenced with 150 bp paired end reads on an Illumina NovaSeq 600, generating 1.29 billion reads. Raw reads were trimmed for quality and adapter contamination using Trimmomatic V0.36[68] where leading and

364 trailing quality was set at 2, sliding window length was 4 with a quality of 2, and minimum
365 length was 31.
366
367 To quantify genetic variation, SuperTranscripts were generated from the reference transcriptome
368 [69] using the Trinity_gene_splice_modeler.py command in the Trinity pipeline [70].
369 SuperTranscripts act as a reference by collapsing isoforms into a single transcript, which enables
370 variant detection without a reference genome [71]. Trimmed reads were aligned to the
371 SuperTranscripts using bwa mem [72]. After filtering, we identify 322,595 variant sites among all
372 replicates.
373
374 Variants were called using VarScan v2.3 [73] (2 alternate reads to call a variant, p-value of 0.1,
375 minimum coverage of 30x, minimum variant allele frequency of 0.01). Following this, variants
376 were stringently filtered to include no missing data, only sites where at least 4 samples were
377 called as variable and each with a minor allele frequency of at least 0.025 (minimum of 1
378 heterozygous individual), any sites with depth greater than 3x the median (median=132x), and
379 sites with a minimum coverage of 50x per sample (2 reads/diploid individual). This reduced
380 called variants from an initial 5,547,802 to 322,595.
381
382 Gene expression was quantified at the gene level as recommended [74] using Salmon v0.10.2 [75]
383 and transcript abundances were converted to gene-level counts using the tximport package in R
384 [76]. The reference transcriptome was indexed using quasi mapping with a k-mer length of 31 and
385 transcripts were quantified while correcting for sequence specific bias and GC bias. We were
386 interested in assessing expression patterns between treatments with each generation and how

these patterns changed through time and, therefore, analyzed each generation separately. Genes with low expression (fewer than 10 counts in more than 90% of the samples) were removed from the dataset. This left 23 324, 24 882, and 24 132 genes for F1, F2, and F3, respectively. Counts were normalized and log transformed using the rlog command in DESeq2 [77].

Gene expression plasticity

DESeq2 was used to identify the number of plastic genes for each line defined as the genes changing expression between environments within a line (GH_{GH} vs. GH_{AM}; AM_{AM} vs. AM_{GH}). For each generation, we required at least 10 counts in 90% of samples. Differentially expressed genes were identified using the model ~Line + Treatment + Line:Treatment and any contrasts were considered significant when adjusted p-values were < 0.05.

Discriminant analysis of principal components

Discriminant analysis of principal components (DAPC) was used to quantify the degree to which gene expression and allele frequencies converged on the adaptive state within each environment. Here, we assume that each line has reached the adaptive optimum after 20 generations. Using the filtered, normalized, and transformed expression data from DeSeq2, shifts in gene expression in transplanted lines across generations were quantified using DAPC in the adegenet package in R [78]. Discriminant functions for each generation were first generated using the non-transplanted lines to identify genes consistently differentially expressed. Transplanted lines were fit to this discriminant function space and used MCMCglmm models in R [79] to model the effect of line origin and transplant on movement in discriminant function space. 2500 posterior estimates were generated and the difference in the transplant effect for each line was quantified by calculating

410 the absolute difference between these estimates. This can be viewed as the difference between
411 the lengths of the lines representing average shifts in Fig. 4. These differences were used to
412 generate a 95% credible interval and the proportion of positive or negative values were
413 considered a p-value for the difference in magnitude of the effect of transplant on each line in
414 discriminant function space.
415
416 DAPC was also used to identify divergence in allele frequency between the AM and GH lines.
417 The same approach as for gene expression (above) was taken where we generated the DAPC
418 with lines in their home environment and then fit transplanted lines to discriminant function
419 space.
420
421 *Adaptive allele frequency and gene expression divergence*
422 To identify loci consistently shifting in response to selection, Cochran–Mantel–Haenszel (CMH)
423 tests were used to identify specific SNPs that were consistently diverged between the AM and
424 GH lines and represent the most likely targets of adaptation. This approach looks for consistent
425 changes in allele frequencies across all replicates and is a common and powerful technique in
426 experimental evolution [35,80]. We calculated CMH p-values for AM_{AM} versus GH_{GH} lines (n = 4,
427 each) for each of the three sampled generations. Significance thresholds ($P < 5.17e-08$) were
428 defined with Bonferroni corrections using the total number of SNPs (322,595) multiplied by
429 three, representing the total number of tests conducted. The SNPs that were identified in all three
430 generations were considered adaptive (Fig. S6). This approach assumes that AM and GH lines
431 have reached their phenotypic optimum and any additional evolution in the F2 or F3 generations

is a product of drift, an assumption that is reasonable given the preceding 20 generations of selection.

DESeq2 was used to identify the specific genes that were adaptive differentially expressed between non-transplanted AM and GH lines at each generation. Using the same geneset and model from DeSeq2, above, we identified differentially expressed genes between AM and GH in their home environment with an adjusted significance threshold of p-values < 0.05.

Quantifying genetic diversity

We estimate genetic diversity (π) for each replicate using Popoolation [81] with 100 bp non-overlapping sliding windows. To quantify if π was differentially lost in any treatment, median π values were compared using an Anova with a Tukey post-hoc test. We next tested if regions containing adaptively divergent loci between non-transplanted GH and AM lines lost π at a different rate than regions containing only neutral variants. The change in π was calculated for each replicate and the change in π for GH_{AM} and AM_{GH} were compared using Wilcoxon Rank Sum tests with bonferroni corrections. Gene ontology enrichment was performed with GO Mann-Whitney U [82], which requires no significance threshold, but takes the change in π for each group and asks if any functional category falls towards the tails of this distribution (in our case, one-sided to identify disproportionately low values). We use this same approach for gene expression and allele frequencies divergence between lines in their home environments. For allele frequencies, the minimum p-value was chosen for each gene.

Finally, we tested for overlap between the allelic and gene expression results to determine if the genes in each were significantly correlated. We correlated the relationship between the -log10 of the CMH p-values for the allele frequencies and the differential gene expression p-values between GH_{GH} and AM_{AM}. This analysis showed the two sets were distinct and the variation explained by each was less than 1% at each generation, indicating that there was minimal bias in estimating allele frequencies due to differentially expressed genes.

References:

1. Rahmstorf, S. & Coumou, D. Increase of extreme events in a warming world. *Proc. Natl. Acad. Sci. U. S. A.* **108**, 17905–17909 (2011).
2. Somero, G. N. The physiology of climate change: how potentials for acclimatization and genetic adaptation will determine 'winners' and 'losers'. *J. Exp. Biol.* (2010).
3. Hoffmann, A. A. & Sgrò, C. M. Climate change and evolutionary adaptation. *Nature* **470**, 479–485 (2011).
4. Chevin, L.-M., Lande, R. & Mace, G. M. Adaptation, plasticity, and extinction in a changing environment: towards a predictive theory. *PLoS Biol.* **8**, e1000357 (2010).
5. Kawecki, T. J. & Ebert, D. Conceptual issues in local adaptation. *Ecol. Lett.* **7**, 1225–1241 (2004).
6. Campbell-Staton, S. C. *et al.* Winter storms drive rapid phenotypic, regulatory, and genomic shifts in the green anole lizard. *Science* **357**, 495–498 (2017).
7. Barrett, R. D. H. *et al.* Linking a mutation to survival in wild mice. *Science* **363**, 499–504 (2019).

8. Therkildsen, N. O. *et al.* Contrasting genomic shifts underlie parallel phenotypic evolution in response to fishing. *Science* **365**, 487–490 (2019).

9. Brennan, R. S., Garrett, A. D., Huber, K. E., Hargarten, H. & Pespeni, M. H. Rare genetic variation and balanced polymorphisms are important for survival in global change conditions. *Proceedings of the Royal Society B: Biological Sciences* **286**, 20190943 (2019).

10. Stearns, S. C. The evolutionary significance of phenotypic plasticity. *Bioscience* (1989).

11. Thompson, J. D. Phenotypic plasticity as a component of evolutionary change. *Trends Ecol. Evol.* **6**, 246–249 (1991).

12. Kelly Morgan. Adaptation to climate change through genetic accommodation and assimilation of plastic phenotypes. *Philos. Trans. R. Soc. Lond. B Biol. Sci.* **374**, 20180176 (2019).

13. Fox Rebecca J., Donelson Jennifer M., Schunter Celia, Ravasi Timothy & Gaitán-Espitia Juan D. Beyond buying time: the role of plasticity in phenotypic adaptation to rapid environmental change. *Philos. Trans. R. Soc. Lond. B Biol. Sci.* **374**, 20180174 (2019).

14. Hendry, A. P. Key Questions on the Role of Phenotypic Plasticity in Eco-Evolutionary Dynamics. *J. Hered.* **107**, 25–41 (2016).

15. Chevin, L. M., Collins, S. & Lefèvre, F. Phenotypic plasticity and evolutionary demographic responses to climate change: taking theory out to the field. *Funct. Ecol.* (2013).

16. Calosi, P., De Wit, P., Thor, P. & Dupont, S. Will life find a way? Evolution of marine species under global change. *Evol. Appl.* **9**, 1035–1042 (2016).

17. Bock, D. G., Kantar, M. B., Caseys, C., Matthey-Doret, R. & Rieseberg, L. H. Evolution of invasiveness by genetic accommodation. *Nat Ecol Evol* **2**, 991–999 (2018).

18. Scoville, A. G. & Pfrender, M. E. Phenotypic plasticity facilitates recurrent rapid adaptation to introduced predators. *Proc. Natl. Acad. Sci. U. S. A.* **107**, 4260–4263 (2010).

19. Corl, A. *et al.* The Genetic Basis of Adaptation following Plastic Changes in Coloration in a Novel Environment. *Curr. Biol.* **28**, 2970–2977.e7 (2018).

20. Schaum C. Elisa & Collins Sinéad. Plasticity predicts evolution in a marine alga. *Proceedings of the Royal Society B: Biological Sciences* **281**, 20141486 (2014).

21. Perry, B. W., Schield, D. R. & Castoe, T. A. Evolution: Plasticity versus Selection, or Plasticity and Selection? *Current biology: CB* vol. 28 R1104–R1106 (2018).

22. Via, S. & Lande, R. Genotype-Environment Interaction and the Evolution of Phenotypic Plasticity. *Evolution* **39**, 505–522 (1985).

23. Chevin, L.-M. & Lande, R. When do adaptive plasticity and genetic evolution prevent extinction of a density-regulated population? *Evolution* **64**, 1143–1150 (2010).

24. Ghalambor, C. K., McKAY, J. K., Carroll, S. P. & Reznick, D. N. Adaptive versus non-adaptive phenotypic plasticity and the potential for contemporary adaptation in new environments. *Funct. Ecol.* **21**, 394–407 (2007).

25. Williams, S. E., Shoo, L. P., Isaac, J. L., Hoffmann, A. A. & Langham, G. Towards an integrated framework for assessing the vulnerability of species to climate change. *PLoS Biol.* **6**, 2621–2626 (2008).

26. Helmuth, B. *et al.* Long-term, high frequency in situ measurements of intertidal mussel bed temperatures using biomimetic sensors. *Sci Data* **3**, 160087 (2016).

27. Feely, R. A., Sabine, C. L., Hernandez-Ayon, J. M., Ianson, D. & Hales, B. Evidence for upwelling of corrosive 'acidified' water onto the continental shelf. *Science* **320**, 1490–1492 (2008).

523 28. Humes, A. G. How many copepods? in *Ecology and Morphology of Copepods* 1–7
524 (Springer Netherlands, 1994).
525 29. Langer, J. A. F. *et al.* Acclimation and adaptation of the coastal calanoid copepod Acartia
526 tonsa to ocean acidification: a long-term laboratory investigation. *Mar. Ecol. Prog. Ser.*
527 **619**, 35–51 (2019).
528 30. Kelly, M. W., Pankey, M. S., DeBiasse, M. B. & Plachetzki, D. C. Adaptation to heat stress
529 reduces phenotypic and transcriptional plasticity in a marine copepod. *Funct. Ecol.* **31**, 398–
530 406 (2017).
531 31. Dam, H. G. Evolutionary adaptation of marine zooplankton to global change. *Ann. Rev.*
532 *Mar. Sci.* **5**, 349–370 (2013).
533 32. Sunday, J. M. *et al.* Evolution in an acidifying ocean. *Trends Ecol. Evol.* **29**, 117–125
534 (2014).
535 33. Reusch, T. B. H. & Boyd, P. W. Experimental evolution meets marine phytoplankton.
536 *Evolution* **67**, 1849–1859 (2013).
537 34. Merilä, J. & Hendry, A. P. Climate change, adaptation, and phenotypic plasticity: the
538 problem and the evidence. *Evol. Appl.* **7**, 1–14 (2014).
539 35. Schlötterer, C., Kofler, R., Versace, E., Tobler, R. & Franssen, S. U. Combining
540 experimental evolution with next-generation sequencing: a powerful tool to study
541 adaptation from standing genetic variation. *Heredity* **114**, 431–440 (2015).
542 36. Munday, P. L., Warner, R. R., Monro, K., Pandolfi, J. M. & Marshall, D. J. Predicting
543 evolutionary responses to climate change in the sea. *Ecol. Lett.* **16**, 1488–1500 (2013).
544 37. Mauchline, J. *The Biology of Calanoid Copepods*. (Academic Press, 1998).
545 38. Steinberg, D. K. & Landry, M. R. Zooplankton and the Ocean Carbon Cycle. *Ann. Rev.*

546 *Mar. Sci.* **9**, 413–444 (2017).

547 39. Gobler, C. J. & Baumann, H. Hypoxia and acidification in ocean ecosystems: coupled
548 dynamics and effects on marine life. *Biol. Lett.* **12**, (2016).

549 40. Rice, E., Dam, H. G. & Stewart, G. Impact of Climate Change on Estuarine Zooplankton:
550 Surface Water Warming in Long Island Sound Is Associated with Changes in Copepod Size
551 and Community Structure. *Estuaries Coasts* **38**, 13–23 (2015).

552 41. IPCC. *Climate Change 2014: Mitigation of Climate Change. Contribution of Working*
553 *Group III to the Fifth Assessment Report of the Intergovernmental Panel on Climate*
554 *Change*. vol. 1454 (2014).

555 42. Caldeira, K. & Wickett, M. E. Oceanography: anthropogenic carbon and ocean pH. *Nature*
556 **425**, 365 (2003).

557 43. Behrenfeld, M. J. *et al.* Climate-driven trends in contemporary ocean productivity. *Nature*
558 **444**, 752–755 (2006).

559 44. Caswell, H. Matrix population models. *Encyclopedia of Environmetrics* **3**, (2006).

560 45. Pedersen, S. A. *et al.* Multigenerational exposure to ocean acidification during food
561 limitation reveals consequences for copepod scope for growth and vital rates. *Environ. Sci.*
562 *Technol.* **48**, 12275–12284 (2014).

563 46. Mayor, D. J., Sommer, U., Cook, K. B. & Viant, M. R. The metabolic response of marine
564 copepods to environmental warming and ocean acidification in the absence of food. *Sci.*
565 *Rep.* **5**, 13690 (2015).

566 47. Healy, T. M., Brennan, R. S., Whitehead, A. & Schulte, P. M. Tolerance traits related to
567 climate change resilience are independent and polygenic. *Glob. Chang. Biol.* (2018)
568 doi:10.1111/gcb.14386.

569 48. Rose, N. H., Bay, R. A., Morikawa, M. K. & Palumbi, S. R. Polygenic evolution drives
570 species divergence and climate adaptation in corals. *Evolution* **72**, 82–94 (2018).
571 49. Fuller, Z. L. *et al.* Population genetics of the coral Acropora millepora: Toward genomic
572 prediction of bleaching. *Science* **369**, (2020).
573 50. Belhadj Slimen, I. *et al.* Reactive oxygen species, heat stress and oxidative-induced
574 mitochondrial damage. A review. *Int. J. Hyperthermia* **30**, 513–523 (2014).
575 51. Downs, C. A. & Heckathorn, S. A. The mitochondrial small heat-shock protein protects
576 NADH:ubiquinone oxidoreductase of the electron transport chain during heat stress in
577 plants. *FEBS Lett.* **430**, 246–250 (1998).
578 52. Mathew, A. N. U. & Morimoto, R. I. Role of the heat-shock response in the life and death
579 of proteins. *Ann. N. Y. Acad. Sci.* **851**, 99–111 (1998).
580 53. Evans, T. G., Pespeni, M. H., Hofmann, G. E., Palumbi, S. R. & Sanford, E. Transcriptomic
581 responses to seawater acidification among sea urchin populations inhabiting a natural pH
582 mosaic. *Mol. Ecol.* **26**, 2257–2275 (2017).
583 54. Bailey, A. *et al.* Regulation of gene expression is associated with tolerance of the Arctic
584 copepod *Calanus glacialis* to CO_2-acidified sea water. *Ecol. Evol.* **7**, 7145–7160 (2017).
585 55. Anjum, R. & Blenis, J. The RSK family of kinases: emerging roles in cellular signalling.
586 *Nat. Rev. Mol. Cell Biol.* **9**, 747–758 (2008).
587 56. Murren, C. J. *et al.* Constraints on the evolution of phenotypic plasticity: limits and costs of
588 phenotype and plasticity. *Heredity* **115**, 293–301 (2015).
589 57. Bay, R. A. *et al.* Genomic signals of selection predict climate-driven population declines in
590 a migratory bird. *Science* **359**, 83–86 (2018).
591 58. Bay, R. A. *et al.* Predicting responses to contemporary environmental change using

592 evolutionary response architectures. *Am. Nat.* **189**, 463–473 (2017).

593 59. Bush, A. *et al.* Incorporating evolutionary adaptation in species distribution modelling
594 reduces projected vulnerability to climate change. *Ecol. Lett.* **19**, 1468–1478 (2016).

595 60. Valladares, F. *et al.* The effects of phenotypic plasticity and local adaptation on forecasts of
596 species range shifts under climate change. *Ecol. Lett.* **17**, 1351–1364 (2014).

597 61. Vehmaa, A., Brutemark, A. & Engström-Öst, J. Maternal effects may act as an adaptation
598 mechanism for copepods facing pH and temperature changes. *PLoS One* **7**, e48538 (2012).

599 62. Feinberg, L. R. & Dam, H. G. Effects of diet on dimensions, density and sinking rates of
600 fecal pellets of the copepod Acartia tonsa. *Mar. Ecol. Prog. Ser.* **175**, 87–96 (1998).

601 63. Murray, C. S. & Baumann, H. You better repeat it: complex CO2× temperature effects in
602 Atlantic silverside offspring revealed by serial experimentation. *Diversity* **10**, 69 (2018).

603 64. Therneau, T. M. & Grambsch, P. M. *Modeling Survival Data: Extending the Cox Model*.
604 (Springer, 2013).

605 65. Therneau, T. A Package for Survival Analysis in S. version 2.38. (2015).

606 66. Kassambara, A., Kosinski, M. & Biecek, P. survminer: Drawing Survival Curves using
607 ggplot2. **1**, (2017).

608 67. Houde, S. E. L. & Roman, M. R. Effects of food quality on the functional ingestion
609 response of the copepod Acartia tonsa. *Mar. Ecol. Prog. Ser.* **40**, 69–77 (1987).

610 68. Bolger, A. M., Lohse, M. & Usadel, B. Trimmomatic: a flexible trimmer for Illumina
611 sequence data. *Bioinformatics* **30**, 2114–2120 (2014).

612 69. Jørgensen, T. S. *et al.* The genome and mRNA transcriptome of the cosmopolitan calanoid
613 copepod Acartia tonsa Dana improve the understanding of copepod genome size evolution.
614 *Genome Biol. Evol.* (2019) doi:10.1093/gbe/evz067.

615 70. Haas, B. J. *et al.* De novo transcript sequence reconstruction from RNA-seq using the
616 Trinity platform for reference generation and analysis. *Nat. Protoc.* **8**, 1494–1512 (2013).
617 71. Davidson, N. M., Hawkins, A. D. K. & Oshlack, A. SuperTranscripts: a data driven
618 reference for analysis and visualisation of transcriptomes. *Genome Biol.* **18**, 148 (2017).
619 72. Li, H. Aligning sequence reads, clone sequences and assembly contigs with BWA-MEM.
620 *arXiv preprint arXiv:1303.3997* (2013).
621 73. Koboldt, D. C. *et al.* VarScan 2: somatic mutation and copy number alteration discovery in
622 cancer by exome sequencing. *Genome Res.* **22**, 568–576 (2012).
623 74. Soneson, C., Love, M. I. & Robinson, M. D. Differential analyses for RNA-seq: transcript-
624 level estimates improve gene-level inferences. *F1000Res.* **4**, (2016).
625 75. Patro, R., Duggal, G., Love, M. I., Irizarry, R. A. & Kingsford, C. Salmon provides fast and
626 bias-aware quantification of transcript expression. *Nat. Methods* **14**, 417–419 (2017).
627 76. R Core Team. R: A Language and Environment for Statistical Computing. (2019).
628 77. Love, M. I., Huber, W. & Anders, S. Moderated estimation of fold change and dispersion
629 for RNA-seq data with DESeq2. *Genome Biol.* **15**, 550 (2014).
630 78. Jombart, T. & Ahmed, I. adegenet 1.3-1: new tools for the analysis of genome-wide SNP
631 data. *Bioinformatics* (2011) doi:10.1093/bioinformatics/btr521.
632 79. Hadfield, J. D. MCMC Methods for Multi-Response Generalized Linear Mixed Models:
633 The MCMCglmm R Package. *Journal of Statistical Software* vol. 33 1–22 (2010).
634 80. Orozco-terWengel, P. *et al.* Adaptation of *Drosophila* to a novel laboratory environment
635 reveals temporally heterogeneous trajectories of selected alleles. *Mol. Ecol.* **21**, 4931–4941
636 (2012).
637 81. Kofler, R. *et al.* PoPoolation: a toolbox for population genetic analysis of next generation

638 sequencing data from pooled individuals. *PLoS One* **6**, e15925 (2011).

639 82. Wright, R. M., Aglyamova, G. V., Meyer, E. & Matz, M. V. Gene expression associated
640 with white syndromes in a reef building coral, Acropora hyacinthus. *BMC Genomics* **16**,
641 371 (2015).

642

643 **Acknowledgments:** We thank Lydia Norton and Gihong Park for culture maintenance and
644 experimental help. RSB appreciates the sponsorship from Maile Neel as a Visiting Research
645 Scientist in the Department of Plant Science & Landscape Architecture at the University of
646 Maryland College Park. **Funding:** This work was funded by the National Science Foundation
647 grants to M.H.P. (OCE 1559075) and H.G.D, H.B. and M.F. (OCE 1559180); **Author**
648 **contributions:** Conceptualization and experimental design: all authors; Experimental execution:
649 JAD; Data collection and analysis: RSB and JAD; Writing-original draft: RSB and MHP;
650 Writing-review and editing: all authors; **Competing interests:** Authors declare no competing
651 interests; **Data and materials availability:** Raw sequence data is available at NCBI BioProject
652 PRJNA555881. Life history data are available as a supplemental file and allele frequency and
653 gene expression table is available on Figshare (https://doi.org/10.6084/m9.figshare.10301690).
654 Correspondence and requests for materials should be addressed to RSB (reid.brennan@uvm.edu)
655 or MHP (mpespeni@uvm.edu). Code to reproduce all analyses can be found at:
656 https://github.com/PespeniLab/tonsa_reciprocal_transplant

657

658 **Extended data:**

659 Figures S1-S8

660 Tables S1-S7

661 **Figures:**

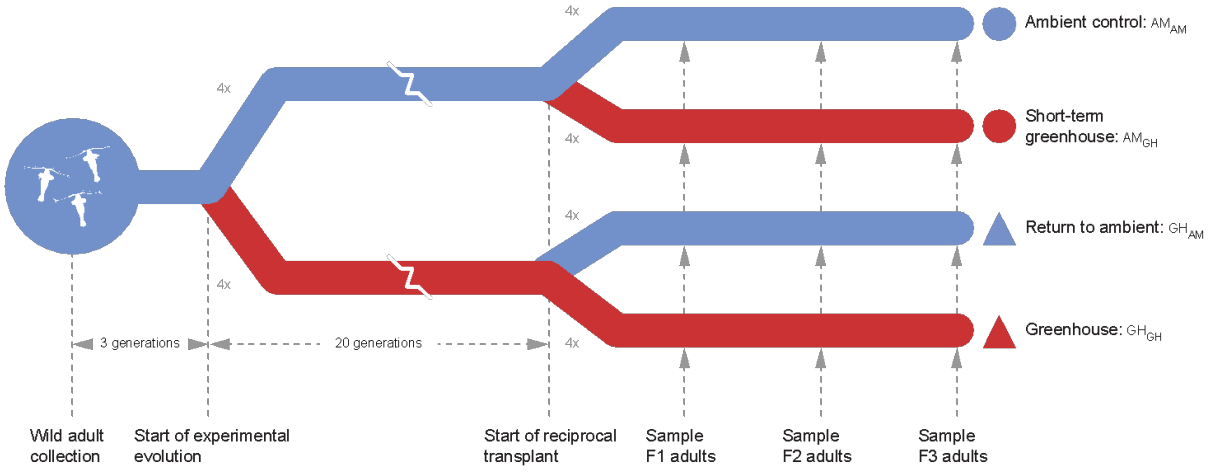

662

663 **Figure 1:** Schematic of the experimental design. Blue lines are ambient (AM) pH and
664 temperature that represent current conditions (pCO_2: 400 ppm; temperature: 18ºC). Red lines are
665 simulated future greenhouse (GH) conditions (pCO_2: 2000 ppm; 22ºC). Adults *Acartia tonsa*
666 were collected from the wild and reared in the lab for three generations. 600 laboratory-
667 acclimated adults seeded each of four replicates at AM and GH conditions where they were
668 reared for 20 generations. At generation 20, each replicate was split into two, where one half was
669 transplanted into the same conditions as the previous 20 generations (AM_{AM}, GH_{GH}) and the
670 other was reciprocally transplanted to the opposite condition (AM_{GH}, GH_{AM}). These transplanted
671 lines were reared for 3 additional generations and sampled for genomics and life-history traits at
672 each generation.

673

674

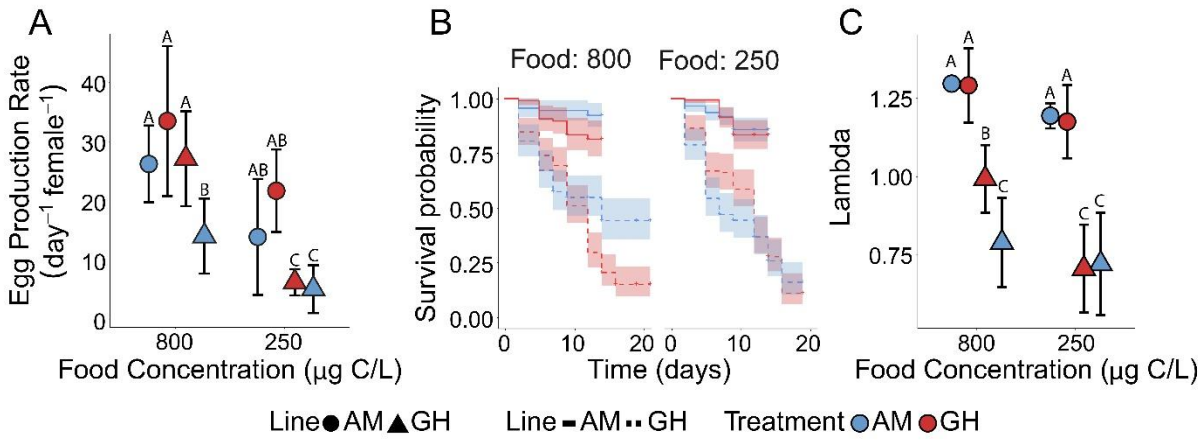

675

676 **Figure 2.** Responses to selection after 20 generations of selection for ambient (AM) and
677 greenhouse (GH) conditions. For all panels, shape indicates selection line, color indicates
678 environmental condition at that generation, and error bars represent 95% confidence intervals. A)
679 Egg production under ad-libitum and lowered food. B) Survivorship under ad-libitum and
680 lowered food. C) Lambda (net reproductive rate) calculated from combined fecundity,
681 development rate, and survivorship data. Capital letters in A and C represent statistical similar
682 groups.

683

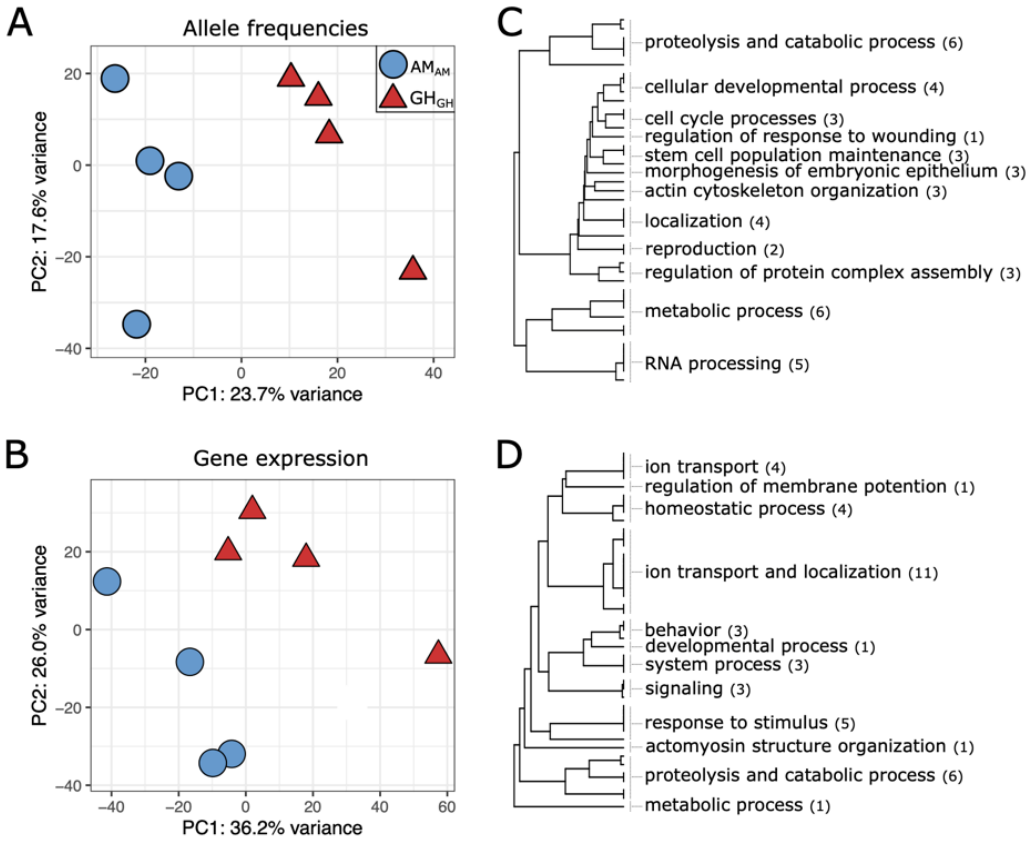

684

685

686 **Figure 3.** Allele frequency and gene expression divergence after 20 generations of selection.
687 Principle component analysis of (A) genome-wide variation in allele frequencies and (B) gene
688 expression at the F1 generation. (C, D) Gene ontology enrichment results from GO Mann-
689 Whitney U based on p-values from Cochran–Mantel–Haenszel tests (allele frequencies, C) and
690 DeSeq2 (gene expression, D). Gene categories are collapsed for visualization purposes with the
691 number of categories indicated in parentheses. See tables S1-2 and figs. S7-8 for full results.

692

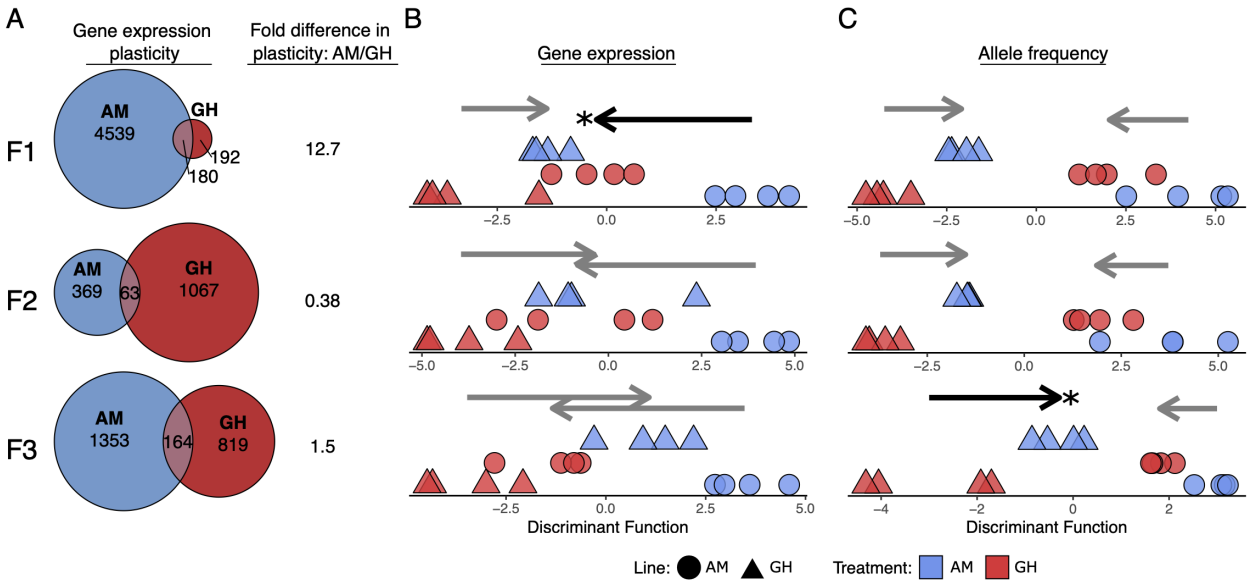

693

694 **Figure 4.** Plastic responses to reciprocal transplant. (A) Gene expression plasticity for AM and
695 GH transplanted lines as defined by differentially expressed genes within a line following
696 transplant (GH_{GH} vs. GH_{AM}; AM_{AM} vs. AM_{GH}). Genome-wide variation in (A) gene expression
697 and (B) allele frequencies across generations. The x-axis shows the discriminant function space
698 that maximizes differences between lines in their home environments. Shape indicates selection
699 line, color indicates treatment condition. The arrows above the points show the mean change for
700 each line after transplant where significantly different shifts are represented by black lines and
701 asterisks. Gene expression profiles match the environment to a greater extent for AM as
702 compared to GH lines at F1 ($P_{MCMC} = 0.03$) but lines show similar movement at F2 and F3
703 ($P_{MCMC} > 0.05$). Conversely, allele frequencies change to a greater degree in the GH line than the
704 AM line by generation F3, indicative of adaptive evolution ($P_{MCMC} = 0.02$).

705

706

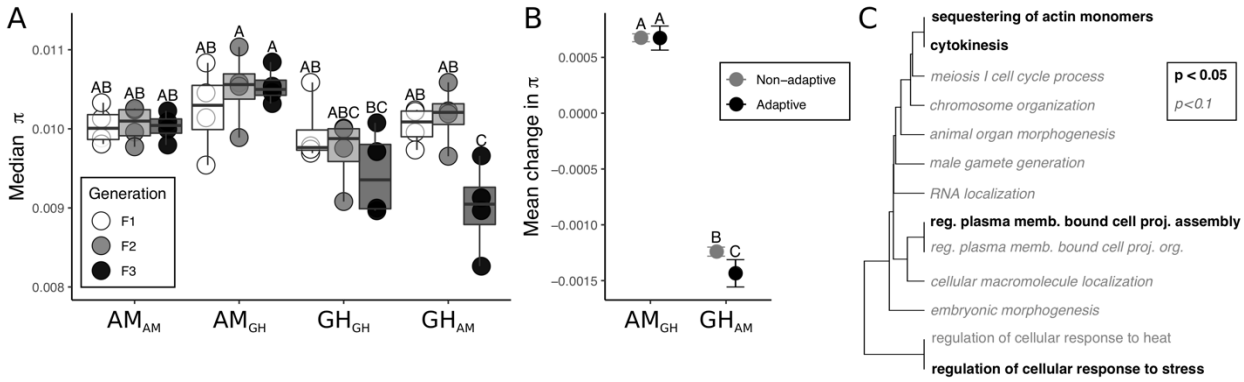

707

708 **Figure 5.** Costs of adaptation. (A) Median nucleotide diversity (π) for all treatments and

709 generations following transplant. (B) Mean change in π from F1 to F3 after transplant for

710 adaptive and non-adaptive SNPs. Letters above each point (for A and B) show significance;

711 points sharing letters are not significantly different. (C) Gene ontology enrichment for the loss of

712 genetic diversity of GH_{AM} at transplant F3; AM_{GH} showed no enrichment.

Supplemental Information

Additional analyses were run to validate the results observed in Fig. 4, where gene expression converged on the adaptive profile across generations, but allele frequencies shifted only in GH_{AM}. We considered expression patterns in the home environment as the adaptive transcriptomic profile for that environment, achieved either through plastic or evolutionary mechanisms (x-axes of Fig. S5A). These adaptive transcriptional profiles were compared to the change in gene expression of a line in transplanted versus long-term selected conditions (y-axes of Fig. S5A). This comparison of long- versus short-term responses across three successive generations allowed us to test if copepods transplanted to the opposite environment can match expression patterns to the long-term, adapted profile. A correlation between long-term, adapted expression (x-axis) and transplant expression change (y-axis) indicates the degree to which transplanted lines can match their expression to the optimal profile for the environmental condition, where a positive correlation represents adaptive changes in expression [1]. After one generation in transplant conditions, gene expression was positively correlated with the adaptive expression for both lines, AM transplanted to GH and GH transplanted to AM (Fig. S5A top panel; $\rho_{AM} = 0.57$, $\rho_{GH} = 0.64$, $P < 0.001$) and this correlation increased each successive generation. Discriminant analysis of principal components (DAPC) showed the same convergence on the adaptive transcriptomic profile (Fig. S5). In accord, the proportion of positively correlated, adaptively expressed genes (dark points; Fig.S5A) increased across generations for both ambient and greenhouse lines ($P < 0.05$; Proportions: $F1_{AM} = 0.85$, $F2_{AM} = 0.87$, $F3_{AM} = 0.90$, $F1_{GH} = 0.66$, $F2_{GH} = 0.94$, $F3_{GH} = 0.95$) with the greatest response in greenhouse relative to ambient lines, 29% versus 5% increase in the proportion adaptive. arriving at 90-95% adaptive gene expression profiles.

We assessed the degree of adaptive evolution for each transplanted line across the generations by quantifying the change in allele frequencies of adaptive loci in transplanted lines. We consider the adaptive difference in allele frequencies as the difference between mean frequencies of AM and GH lines (for the significant loci identified with the CMH test across all generations) and assess the convergence of transplanted lines on this adaptive difference (i.e., do AM in GH frequencies converge on the GH allele frequency?). Spearman's correlation was used to

determine the extent to which these frequencies were correlated. We compared the mean difference in allele frequency between GH_{GH} and AM_{AM} for 17,720 loci that had evolved consistent divergence in allele frequency (x-axes of Fig. S5B) to the mean difference in allele frequency in response to transplant conditions (GH_{am} AM_{GH}; GH_{AM} AM_{GH}; y-axes of Fig. S5B). GH_{AM} copepods evolved to match allele frequencies of the ambient adaptive alleles with increasing changes in frequencies across each successive generation (Fig. S5B). In contrast, AM_{GH} lines did not undergo the same rapid adaptation but maintained allele frequencies (Fig. S5B), even though their transcriptional profiles shifted to match greenhouse adaptive expression (Fig. 3A). Likewise, the proportion of adaptive alleles (dark points) increased across transplant generations for the greenhouse lines, but not the ambient lines (Fig. 3B; proportions test: $P < 0.001$; Proportions: $F1_{AM} = 0.68$, $F2_{AM} = 0.64$, $F3_{AM} = 0.65$; $F1_{GH} = 0.68$, $F2_{GH} = 0.75$, $F3_{GH} = 0.76$).

We realize that criticism has been leveraged against past work that has used similar analyses as in Fig. S5 where the x and y axes share a denominator are not independent [2,3]. This should lead to a positive correlation between the variables, as we observe here. Despite this, there is no reason to expect a consistent change in this correlation across generations as we observe for both the gene expression and allele frequency analysis. Therefore, while some proportion of the positive correlations we observe is due to statistical bias, the increase indicates that lines are shifting gene expression and allele frequency (in AM only) to match their transplanted environment, in agreement with the DAPC in the main text (Fig. 4).

We also acknowledge the presence of a degree of pseudoreplication in the design where each environmental condition is housed in a single incubator [4]. That is, some degree of the responses observed here may be due to specific incubator effects rather than experimental conditions. However, there has been criticism of the idea that shared spatial arrangements between treatments, such as a room or an incubator, necessarily result in statistical dependencies [5,6]. In our case, both CO_2 and temperature were held constant throughout the experiment, continuously monitored, and verified by independent measures (Table S7). We also know that 22 °C is 4 degrees beyond the optimum of 18 °C and results in significant mortality [7]. Finally, the transcriptomic and genomic effects we observe are consistent with both high temperature and

low pH stress. Therefore, while we cannot completely rule out incubator specific effects, it is likely that the majority of the responses observed are due to the experimental treatments.

References

1. Li, L. *et al.* Divergence and plasticity shape adaptive potential of the Pacific oyster. *Nature Ecology & Evolution* 1 (2018).
2. Mallard, F., Jakšić, A. M. & Schlötterer, C. Contesting the evidence for non-adaptive plasticity. *Nature* **555**, E21–E22 (2018).
3. Ho, W.-C. & Zhang, J. Genetic Gene Expression Changes during Environmental Adaptations Tend to Reverse Plastic Changes Even after the Correction for Statistical Nonindependence. *Mol. Biol. Evol.* **36**, 604–612 (2019).
4. Hurlbert, S. H. Pseudoreplication and the Design of Ecological Field Experiments. *Ecol. Monogr.* **54**, 187–211 (1984).
5. Schank, J. C. & Koehnle, T. J. Pseudoreplication is a pseudoproblem. *J. Comp. Psychol.* **123**, 421–433 (2009).
6. Oksanen, L. Logic of experiments in ecology: is pseudoreplication a pseudoissue? *Oikos* **94**, 27–38 (2001).
7. Sasaki, M. C. & Dam, H. G. Integrating patterns of thermal tolerance and phenotypic plasticity with population genetics to improve understanding of vulnerability to warming in a widespread copepod. *Glob. Chang. Biol.* **25**, 4147–4164 (2019).

Table S1: Gene ontology enrichment results for gene expression.

Table S2: Gene ontology enrichment results allele frequency data

Table S3: Gene ontology enrichment for the change in genetic diversity following transplant of GH to AM conditions.

Table S4: Summary table of differential gene expression. AAAA = ambient line in ambient conditions; HHHH = greenhouse in greenhouse conditions; HHAA = ambient in greenhouse conditions; AAHH = greenhouse in ambient conditions. DAPC results are the contribution score for each gene for the DAPC loading. P-values and fold change were calculated with DESeq2.

Table S5: Raw survivorship data from figure 2.

Table S6: Raw fecundity data from figure 2.

Table S7: Environmental variables. Each temperature and CO_2 level used in this experiment was evaluated to ensure that environmental conditions were accurate. SD = standard deviation, N = number of observations, SE = standard error of the mean.

Treatment	Variable	Target value	Mean measured value	SD	N	SE
Ambient	Temperature	18	18.04	0.361	101	0.036
Greenhouse	Temperature	22	21.93	0.339	101	0.034
Ambient	pH	8.2	8.23	0.059	101	0.006
Greenhouse	pH	7.5	7.57	0.070	101	0.007
Ambient	pCO_2	400	387.9	49.85	9	16.62
Greenhouse	pCO_2	2000	2356.2	119.78	9	39.93

Supplemental figures:

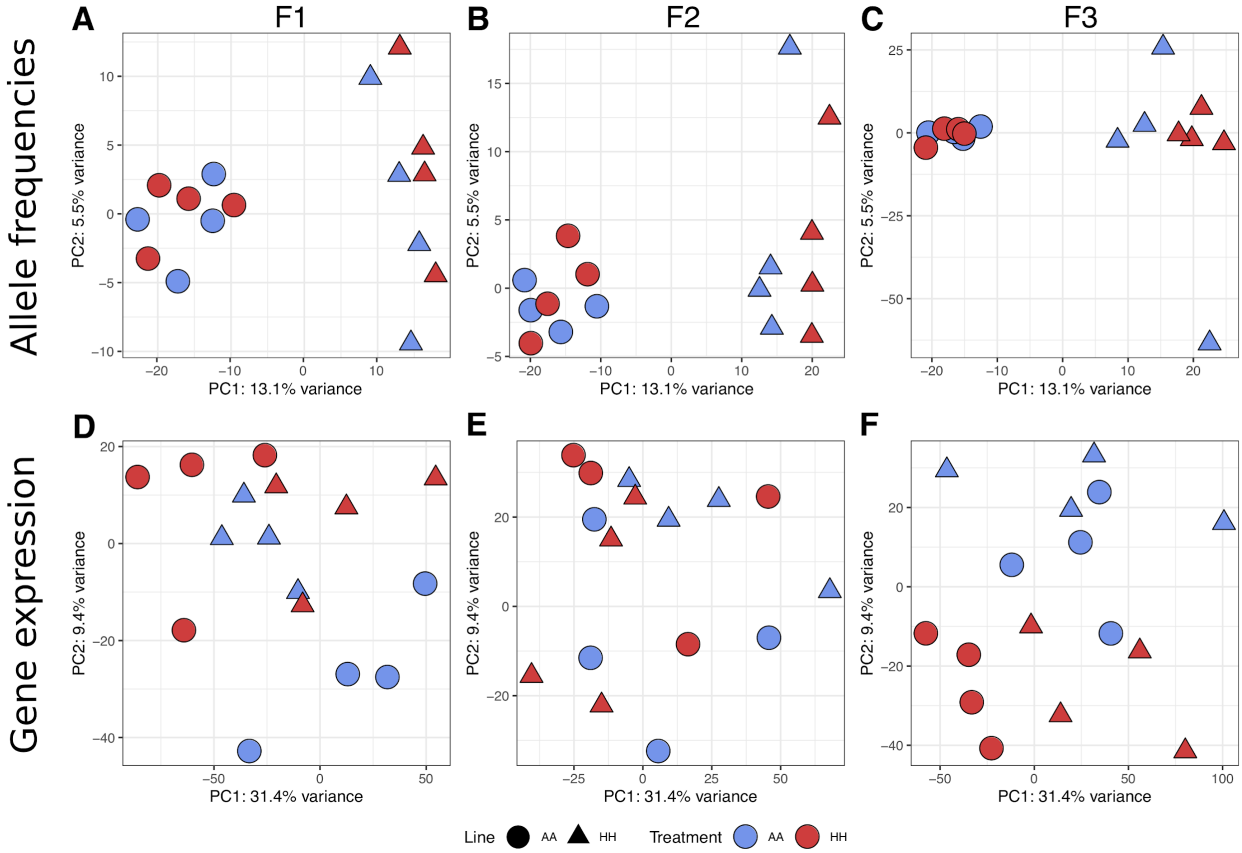

Figure S1: Principal component analysis of genome-wide genetic variation (panels A-C) and gene expression patterns (panels D-F) during three generations of reciprocal transplant following 20 generations of selection for ambient (AM) and greenhouse (GH) conditions. Shape indicates selection line and color indicates environmental condition at that generation. Both gene expression and genetic variation clustered by line, rather than condition at F1. By F3, a line effect was evident for both lines' gene expression.

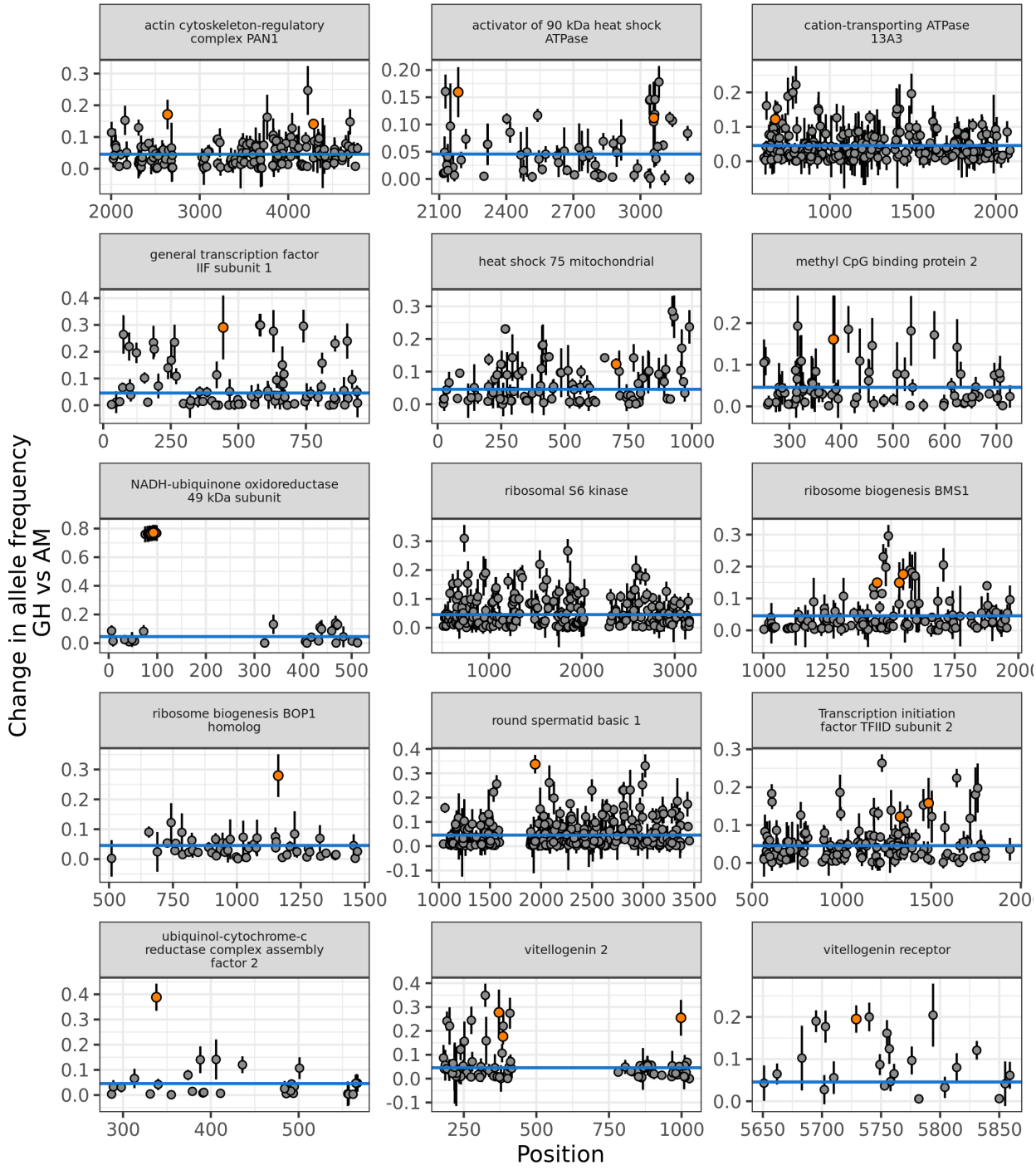

Figure S2: Candidate genes underlying adaptation to GH environments. Points represent the average absolute change in allele frequency between AM_{AM} and GH_{GH} for F1, F2, and F3. Orange points are non-synonymous polymorphisms in the top 10% of allele frequency change distribution. Error bars show standard error between replicates. Note that y-axes are different between plots.

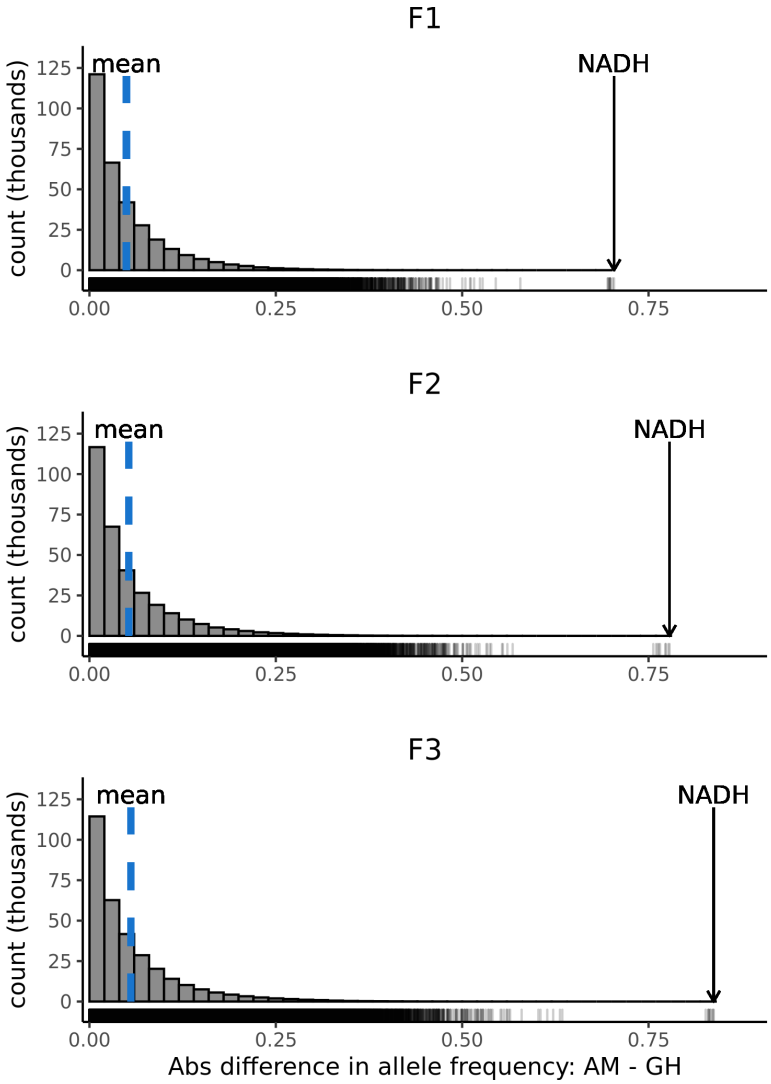

Figure S3: Change in allele frequencies between AM_{AM} and GH_{GH} for all three generations. The blue dashed line indicates the mean frequency change across all loci and the arrow show the extreme frequency change of NADH-ubiquinone oxidoreductase 49 kDa subunit (NDUFS2) at each generation.

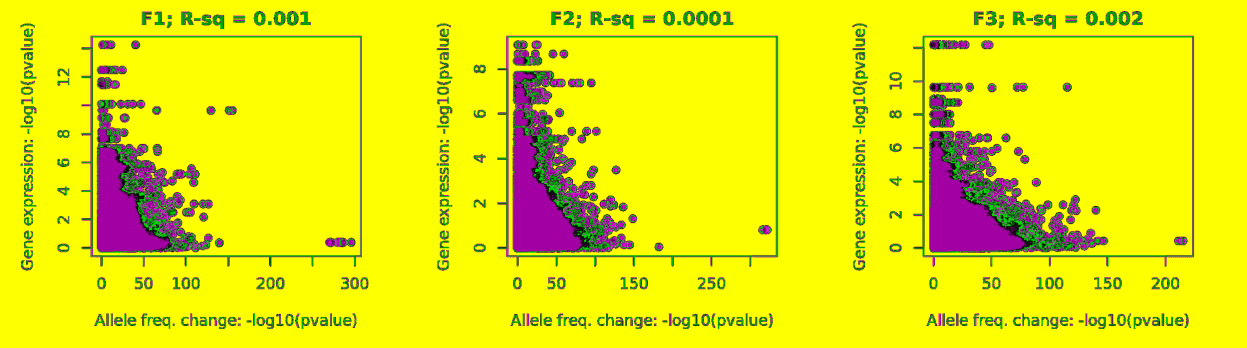

Figure S4: Relationship between gene expression and allele frequency divergence. X-axis is the -log10 of p-values from the CMH between AM and GH in their home conditions. Y-axis corresponds to the -log10 of p-values of expression differences between AM and GH in home conditions. For all generations, the variance explained is low, indicating that gene expression and allele frequency divergence is largely distinct.

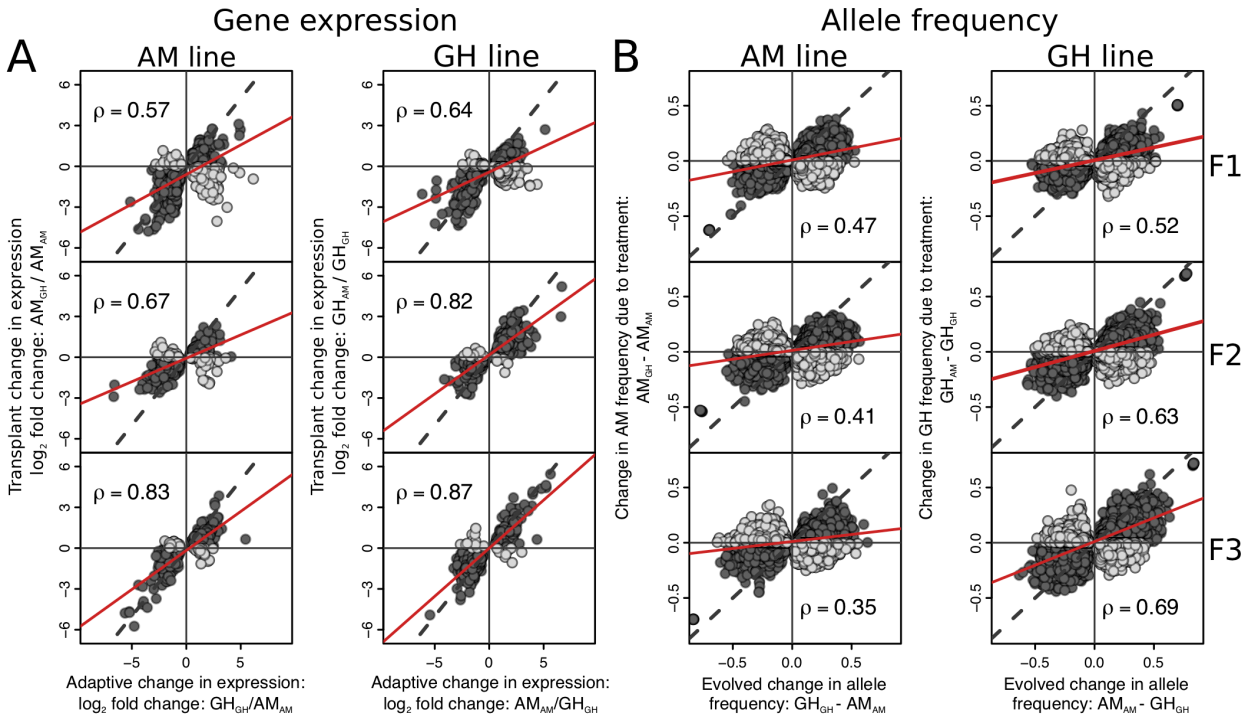

Figure S5: Convergence on evolved differences following transplant. For all plots, the dashed black line is a 1:1 relationship, the solid red line is the observed relationship between the x and y axes. The x-axis is the evolved and adaptive differences between the lines in their home environment. The y-axis compares each line in its transplanted environment to its home environment. Plots illustrate whether transplanted lines converge on the adaptive pattern for a given treatment condition. Dark points show the same pattern as the adaptive difference, light points are in the opposite direction. Pearson's correlation (ρ) is presented for each plot at each generation; generations organized F1 to F3, top to bottom. (A) Evolved changes in gene expression between GH and AM in their home environments (GH_{GH} and AM_{AM}; x-axis) versus the transplant changes in expression (GH_{AM} and AM_{GH}; y-axis) for the same genes. (B) Evolved differences in allele frequency between GH and AM in their home environment (x-axis) versus the change in allele frequency after transplant (y-axis) for the same genes.

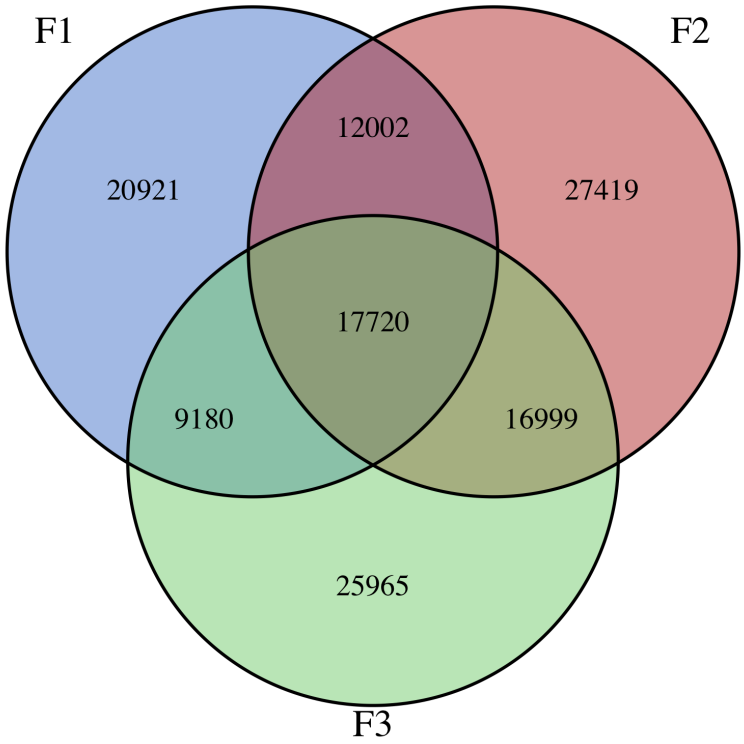

Figure S6: Significant loci ($P < 5.17e\text{-}08$) from CMH tests for each generation between GH_{GH} and AM_{AM}. Loci significant in all three generations were considered targets of selection and adaptive.

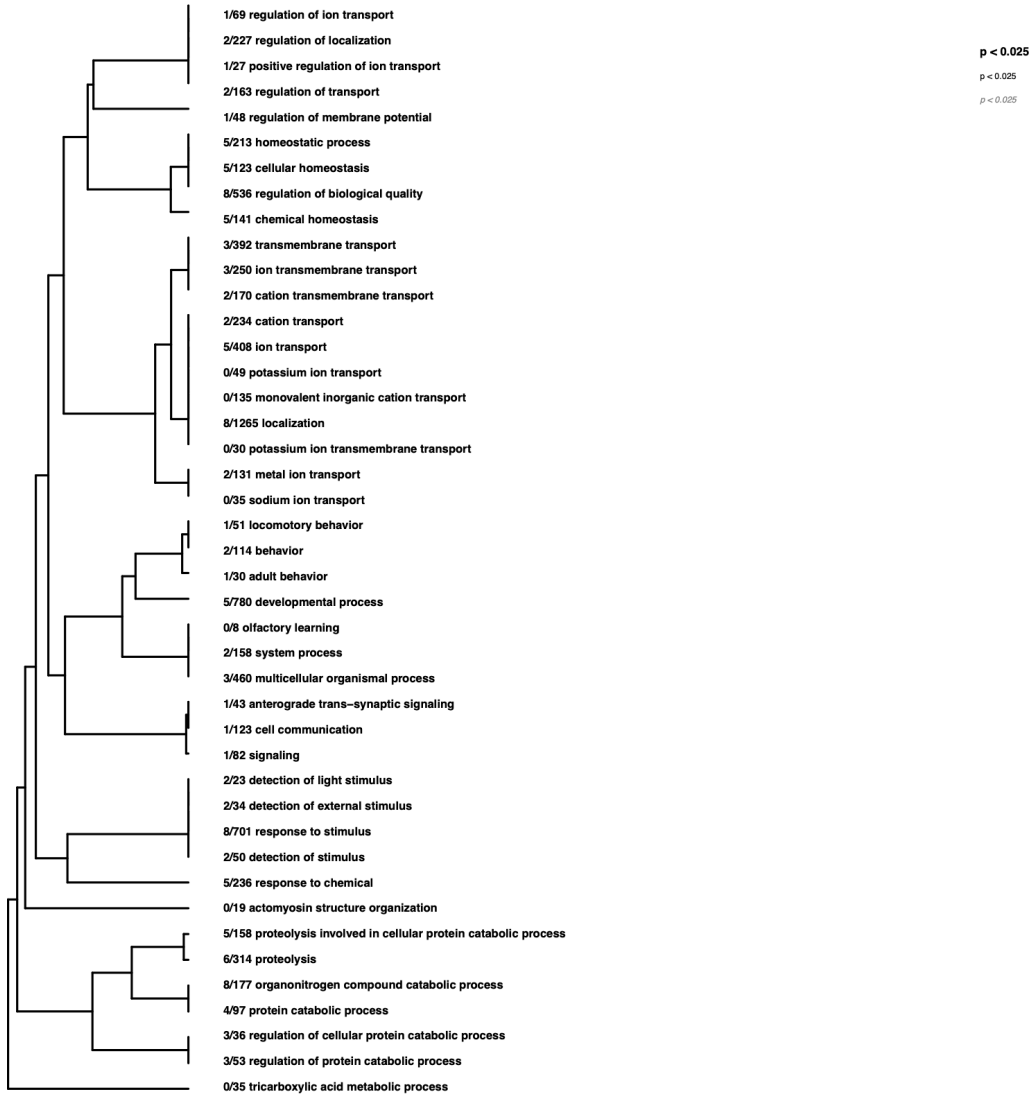

Figure S7: Gene ontology enrichment for allele frequency divergence between AM and GH after 20 generations of selection. This tree represents the full enrichment set in figure 3C.

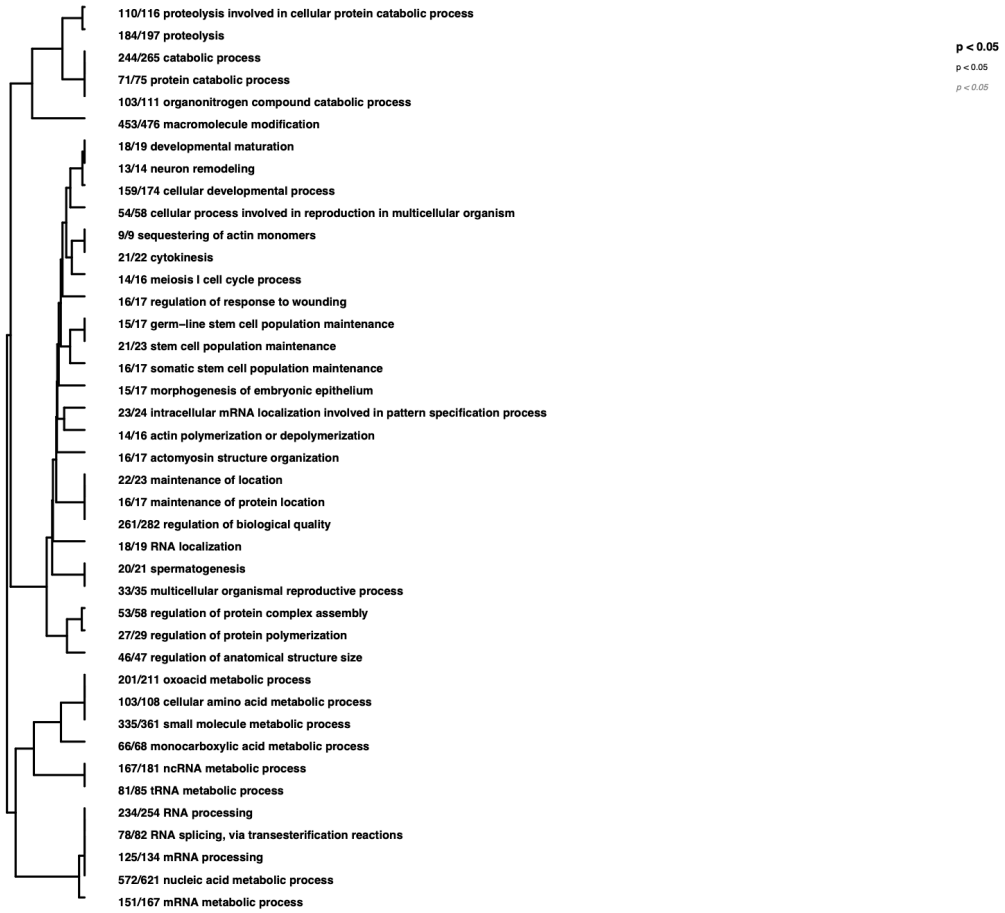

Figure S8: Gene ontology enrichment for gene expression divergence between AM and GH after 20 generations of selection. This tree represents the full enrichment set in figure 3D.